

EDGE-PRESERVATION RESOLUTION ENHANCEMENT WITH ORIENTED WAVELETS

Vladan Velisavljević

Deutsche Telekom Laboratories, Berlin, Germany

ABSTRACT

A novel directionally adaptive image resolution enhancement method is proposed. The method uses a multiple-direction wavelet transform, called *directionlets*, to efficiently extract edge information along different directions, not necessarily horizontal or vertical, from the low-resolution image. Then, the high-resolution image is synthesized using the extracted information to preserve sharpness of edges and texture. The novel algorithm provides the interpolated images at a higher resolution that are better than the images obtained by the state-of-the-art methods in terms of both numeric and visual quality.

Index Terms— Interpolation, directional, directionlet, locally adaptive, wavelet transforms.

1. INTRODUCTION

The problem of resolution enhancement of images commonly refers to generating missing image pixels at high-resolution (HR) from the available low-resolution (LR) image information. This task is often required in magnification, which is an essential part of software zooming, focusing regions of interest, resolution conversion (e.g. in printer drivers), etc. The main challenge is to preserve sharpness of images after resolution enhancement.

The traditional magnification approaches based on bicubic or spline interpolation [1] are used because of fast computation, easy implementation and no *a priori* knowledge assumption. However, these methods generate *blurred* HR images from their LR counterparts. The goal in this paper is to propose a method that reduces this blurring effect at HR.

Several recent methods improve the visual quality of the interpolated images by exploiting the correlation among image pixels and modeling it using the Markov random field either in the wavelet [2, 3] or in the pixel domain [4]. Furthermore, in [4], Li and Nguyen characterize pixels as edge and non-edge and apply different interpolation algorithms to them. Edge-adaptivity and geometric regularity are also exploited in [5] and [6]. In the latter, the edge direction is extracted from the LR covariance matrices and is used to estimate their HR counterparts. However, the computation of the covariance matrices is limited only to the first four neighbor pixels. As a result, the reconstructed edges in the interpolated HR image are still blurred when compared to the edges in the original image.

Another adaptive interpolation method has been proposed in [7]. This method makes use of the multiscale two-dimensional (2-D) wavelet transform (WT) to capture and characterize edges, which induce peaks in the wavelet subbands. The characterization involves estimation of location, magnitude and evolution of the corresponding peaks across wavelet scales determined by the local Lipschitz regularity of edges [8, 9]. This information is used to estimate the corresponding wavelet subbands in the HR multiscale decomposition and to generate the HR image by applying the inverse 2-D WT. The preserved characterization of edges at HR allows for sharpness

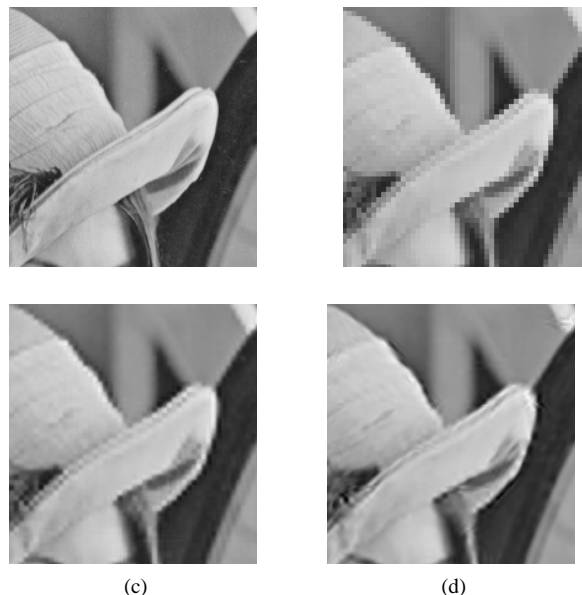


Fig. 1. The image Lena is interpolated using three methods and a magnified detail is shown. (a) The original HR image, (b) bicubic interpolation, (c) locally adaptive wavelet-based interpolation and (d) directionally adaptive interpolation based on directionlets. The novel method based on directionlets outperforms the previous ones providing both higher numeric and visual quality and sharper edges in the interpolated images, especially when locally dominant directions are neither horizontal nor vertical.

and a good visual quality of the reconstructed images. However, notice that the implemented WT is a separable transform constructed only along the *horizontal and vertical directions* [8]. Thus, it fails to characterize efficiently edges along different directions.

Recently, the 2-D WT built along multiple directions (*directionlets*) has been proved [10, 11] to provide sparse representation of images and to improve the performance of wavelet-based image compression methods. This achievement motivates an implementation of directionlets in the interpolation method in [7] to improve the characterization of edges in images along different directions. In the novel interpolation method, proposed here, directionlets are constructed adaptively so that the chosen directions are maximally aligned with locally dominant directions across image. Because of the alignment, the transform generates a sparser representation with a reduced energy in the high-pass wavelet subbands allowing for a more robust estimation of the edge characteristics. The interpolated images have better numeric and visual quality than the images obtained by both the bicubic interpolation and the previous wavelet-based method, as shown in Fig. 1.

The outline of the paper is as follows. The interpolation method proposed by Chang et al. [7] and the basic properties of directionlets are reviewed in Section 2. Then, in Section 3, the novel interpolation

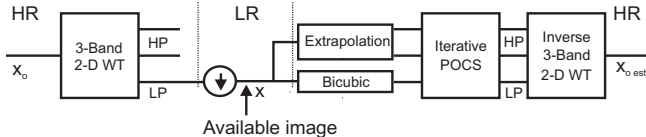


Fig. 2. Block diagram of the interpolation algorithm proposed in [7].

method is presented, with explanation of determination of locally dominant directions and the details of the algorithm. Interpolated images are shown and compared to the previous results in Section 4. Finally, conclusion is given in Section 5.

2. REVIEW OF BACKGROUND WORK

Here, because of lack of space, only a short review of the basic concepts of the interpolation algorithm in [7] and the construction of directionlets [10] is given.

2.1. Locally adaptive wavelet-based interpolation

This algorithm is based on the assumption that the LR version is obtained from the HR original image as a low-pass output of the 3-band 2-D WT (1 low-pass and 2 high-pass subbands), which is also used in [8]. The main idea is to estimate the corresponding missing HR low-pass and two high-pass subbands from the available LR image so that the inverse 3-band 2-D WT applied to these subbands provides a sharp reconstructed HR image (see Fig. 2).

The process of estimation of the 3 wavelet subbands consists of two phases: (a) initial estimate and (b) iterative projections onto convex sets (POCS). In the first phase, the initial estimates of all the 3 subbands at HR are computed. The low-pass subband is simply obtained by the bicubic interpolation of the LR image. However, since the high-pass subbands play an important role in obtaining sharp reconstructed image, they are generated using a more sophisticated method. First, a multiscale 3-band 2-D WT is applied to the LR image with 3 levels of decomposition. Then, extrema of the magnitudes of the wavelet coefficients are located in each row and column of the high-pass subbands to determine the position of sharp variation points (SVP). The extrema of the magnitudes at different scales $j = 1, \dots, J$ related to a single SVP indexed by m follow the scaling relation [8]

$$|W^{(j)} f(x_m)| = K_m 2^{j\alpha_m}, \quad (1)$$

where K_m and α_m are scaling constant and local Lipschitz regularity factor assigned to the m th SVP, respectively. These two parameters are estimated from the determined extrema in the wavelet subbands by linear regression and they are used to extrapolate the corresponding coefficient values in the HR high-pass subbands. The other high-pass coefficients that do not correspond to any SVP are filled by a simple linear interpolation along rows and columns.

In the second phase, the estimated wavelet subbands are iteratively projected onto 3 convex sets determined by the following properties: (a) the 3 wavelet subbands must belong to the subspace of the wavelet transform, (b) the subsampled low-pass subband must be consistent with the LR image and (c) the high-pass subbands must be consistent with the extracted SVP information. The final estimation of the wavelet subbands is transformed back to the original domain using the corresponding inverse 3-band 2-D WT to obtain the interpolated HR image.

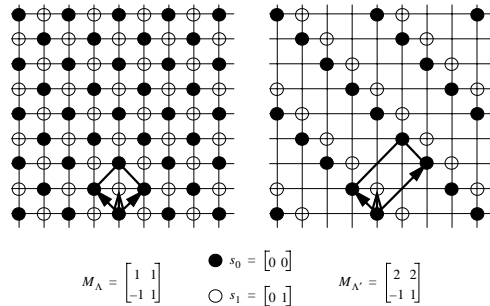


Fig. 3. An example of construction of directionlets based on integer lattices for pair of directions ($45^\circ, -45^\circ$).

2.2. Directionlets

Directionlets are constructed as basis functions of the *skewed anisotropic wavelet transforms* [10]. These transforms make use of integer lattices to apply the scaling and wavelet filtering operations along a pair of directions, not necessarily horizontal or vertical. The basic operations are purely one-dimensional (1-D) and, thus, directionlets retain separability and simplicity of the standard 2-D WT. Fig. 3 shows an example of the construction of directionlets for pair of directions along 45° and -45° . Notice that, even though the originally proposed transform in [10] is critically sampled (the filtering operations are followed by subsampling), here an oversampled version is used by removing the subsampling operations. Such a construction results in a shift-invariant transform with a preserved number of coefficients in each subband, which makes it easy to handle with rotated image rows and columns that have different lengths.

3. DIRECTIONALLY ADAPTIVE INTERPOLATION

The restriction of having only two directions in the construction of directionlets implies a need for spatial segmentation of image and adaptation of the transform directions in each segment. The assigned pairs of transform directions to each segment across the image domain form a *directional map*. The computation of such a map is explained in the sequel.

3.1. Directional map

Image is first divided into spatial segments of the size 16×16 pixels.¹ Directionlets are then applied in each segment along each pair of directions from the set $\mathcal{D} = \{(0^\circ, 90^\circ), (0^\circ, 45^\circ), (0^\circ, -45^\circ), (90^\circ, 45^\circ), (90^\circ, -45^\circ)\}$ using the biorthogonal "9-7" 1-D filterbank [12]. Notice that the pairs of directionlets in the set \mathcal{D} are chosen so that the cubic lattice is not divided into more cosets, as explained in [10] in detail. To avoid a blocking effect in the transform caused by many small segments, the pixels from the neighbor segments are used for filtering across the segment borders.

The best pair of directions $d_n^* \in \mathcal{D}$ is chosen for each segment indexed by n as

$$d_n^* = \arg \min_{d \in \mathcal{D}} \sum_i |W_{n,i}^{(d)}|^2, \quad (2)$$

where the wavelet coefficients $W_{n,i}^{(d)}$ are produced by applying directionlets to the n th segment along the pair d of directions. The directional map determined by the $\{d_n^*\}$ minimizes the energy in the high-pass subbands and provides the best matching between transform and locally dominant directions across segments. For the reason of simplicity of implementation, the pair $(0^\circ, 90^\circ)$ is assigned

¹Different segment sizes do not influence significantly the final results.

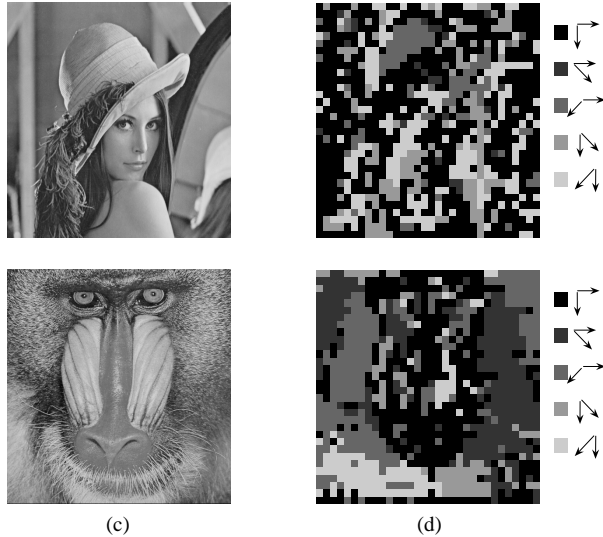


Fig. 4. The transform directions are chosen within each spatial segment of the size 16×16 so that the energy in the high-pass subbands is minimized allowing for the best matching with locally dominant directions in image. The set of chosen directions form the directional map. (a) The original image Lena. (b) The corresponding directional map. (c) The original image Baboon. (d) The corresponding directional map.

by default to smooth segments with no apparent dominant direction (i.e. with low variation of the energy in the high-pass subbands for $d \in \mathcal{D}$). Two examples of directional map are shown in Fig. 4 for the images Lena and Baboon.

The concept of directional map is used in the new interpolation algorithm to improve the extraction of edge information and the estimation of the HR wavelet subbands, as presented next.

3.2. Interpolation algorithm

The proposed novel interpolation algorithm uses the same concept as the previous method in [7] (revisited also in Section 2.1) with several modifications caused by implementation of directionlets instead of the 3-band 2-D WT. Similarly, the goal is, first, to estimate the corresponding wavelet subbands at HR and, then, to apply the inverse transform to obtain a reconstructed HR image.

The estimation of the wavelet subbands also consists of the two phases: (a) initial estimate and (b) iterative POCS. In the initial estimate, the low-pass subband is bicubic-interpolated from the LR image, whereas the high-pass subbands are generated from the extracted SVP information. However, as opposed to the 3-band 2-D WT, directionlets produce three high-pass subbands per scale denoted as HL, LH and HH according to the order of the low-pass and high-pass filtering in the two transform steps. In case of the subbands HL and LH, the search for SVP and the extraction of the SVP parameters are performed along the first and second transform directions, respectively (instead of the horizontal and vertical directions in the previous method), whereas, in case of the subband HH, this process is applied along any of the two directions. Owing to the properties of the applied transform, the extrema of the magnitudes of the directionlets coefficients $|W_s^{(j)} f(x_m)|$ at scales $j = 1, \dots, J$, for $s \in \{\text{HL}, \text{LH}, \text{HH}\}$, follow the scaling relation [9]

$$|W_s^{(j)} f(x_m)| = K_m 2^{j(\alpha_m+1)}, \text{ for } s \in \{\text{HL}, \text{LH}\}, \quad (3)$$

$$|W_s^{(j)} f(x_m)| = K_m 2^{j(2\alpha_m+1)}, \text{ for } s = \text{HH}. \quad (4)$$

By contrast to Chang et al., the SVP parameters (that is, the scaling constant K_m and local Lipschitz regularity factor α_m) are estimated in all the three high-pass subbands by linear regression using (3) and (4), instead of (1).

The initially estimated HR subbands are iteratively refined in the second phase by projection onto three convex sets. The sets are defined by similar properties as in the original algorithm, with a modification for the first set that the subbands must belong to the corresponding subspace of directionlets, instead of the 3-band WT.

Notice that the two SVP parameters that correspond to the same location estimated in different high-pass subbands are correlated, since they are produced by the same SVP. This correlation can be exploited to further improve the estimation of the HR high-pass subbands. However, this issue will be addressed in future work.

The estimated HR subbands are transformed back to the original domain using inverse directionlets and the computed directional map. Notice also that the same transform is used in both the computation of directional map (as explained in Section 3.1) and the initial estimate of the high-pass subbands and, thus, this transform can be applied only once. This fact is exploited to reduce the overall computational complexity to the same order as the complexity of the initial interpolation algorithm. The entire interpolation algorithm is summarized next.

Step 1: Directional map

* Apply directionlets to each 16×16 block using the pairs of transform directions from the set \mathcal{D} and compute the optimal pair of directions using (2),

Step 2: Initial estimate

* Compute the low-pass subband at HR using bicubic interpolation,
 * Determine the SVP in the high-pass subbands using the transform along the directions computed in **Step 1**; estimate the SVP parameters; compute the corresponding high-pass subbands,

Step 3: Iterative POCS (repeat this step K times)²

* Project all the subbands onto the directionlets subspace using a pair of inverse and forward transform,
 * Keep the subsampled version of the low-pass subband consistent with the LR image so that the coefficients at even locations are equal to the original LR pixels,
 * Keep the SVP parameters in the high-pass subbands consistent with the initial edge estimation,

Step 4: Reconstruction

* Apply one step of inverse directionlets on the estimated subbands using the directional map computed in **Step 1**.

4. EXPERIMENTAL RESULTS

The performance of the new method is compared to the performance of both the bicubic interpolation and the previous locally adaptive wavelet-based method from [7] applied to three test images: Lena, Baboon and Kodak star chart. To compare the interpolated images to the reference ones in terms of peak signal-to-noise-ratio (PSNR), the original HR images are first low-pass filtered and subsampled to obtain the LR versions and, then, the resulting images are interpolated back to HR. Furthermore, to emphasize the difference in the visual quality obtained using different interpolation methods, the images are interpolated twice, that is, the resolution at HR is 4 times larger than that at LR. Since the original source code for the method in [7] is not available, it has been rewritten and the obtained PSNRs are approximately close to the results shown in the original paper.

The LR versions of the images Lena and Baboon have 128×128 pixels, whereas the LR version of the image Kodak star chart has

²The results shown in Section 4 are obtained for $K = 5$.

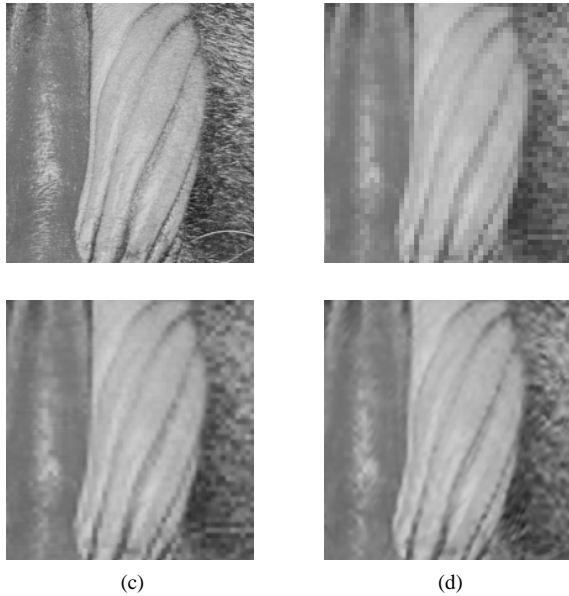


Fig. 5. The image Baboon is interpolated from 128×128 to 512×512 pixels using 3 methods. A magnified area of the image is shown. (a) A detail of the original image shown in Fig. 4(c). (b) Bicubic interpolation. (c) Wavelet-based interpolation. (d) Interpolation with directionlets. Notice that the visual quality of the image interpolated using the novel method is improved as compared to the standard one, even though the numeric improvement is negligible (as presented in Table 1).

Table 1. Results of interpolation of 3 test images using 3 methods: bicubic, wavelet-based and the interpolation based on directionlets.

	Lena	Baboon	Kodak star chart
Bicubic	26.80dB	20.27dB	13.57dB
WT	28.59dB	20.97dB	15.95dB
Directionlets	29.65dB	20.93dB	16.51dB

256×256 pixels. The target HR versions have 512×512 and 1024×1024 pixels, respectively. The images are interpolated using three methods: the bicubic interpolation, the wavelet-based interpolation and the method based on directionlets and the resulting PSNR is shown in Table 1. Notice that the improvement in the numeric quality of interpolation induced by directionlets is significant in case of the images Lena and Kodak star chart, whereas it is rather weak in case of the image Baboon because of a complicated texture. However, the visual quality of the interpolated images is strongly enhanced in all cases as compared to the results of the standard wavelet-based method. To highlight this result, magnified details of all the 3 interpolated images are shown in Fig. 1, 5 and 6. The edges are apparently sharper in the images obtained using the novel method, especially in case when the dominant orientation is neither horizontal nor vertical.

5. CONCLUSIONS

A novel image interpolation algorithm has been obtained by implementation of directionlets in the previously proposed locally adaptive wavelet-based method. The algorithm adapts the transform directions to dominant directions across the image domain and successfully captures oriented features. Moreover, it extracts the information about these features (location, amplitude and Lipschitz de-

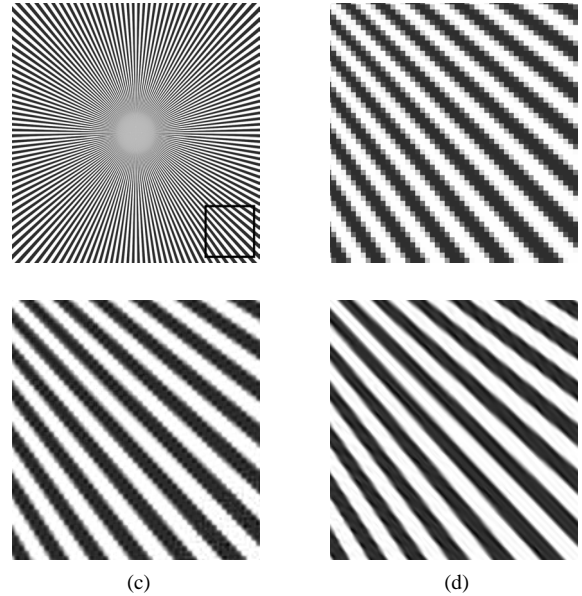


Fig. 6. The image Kodak star chart is interpolated from 256×256 to 1024×1024 pixels using 3 methods. (a) The entire original image with a marked area that is magnified. This area is shown in the interpolated images using (b) bicubic interpolation, (c) wavelet-based interpolation and (d) the interpolation with directionlets. The diagonal lines are reconstructed with the best quality using the novel method.

gree of regularity) from the low-resolution image and uses these parameters to generate a high-resolution version with preserved sharpness. The new method outperforms the previous methods in terms of both numeric and visual quality of reconstructed images. The performance of the method can be even further improved by exploiting the relation of the extracted parameters across the wavelet subbands, which is left for future work.

6. REFERENCES

- [1] P. Thévenaz, T. Blu, and M. Unser, "Interpolation revisited," *IEEE Trans. Med. Imag.*, vol. 19, pp. 739–758, July 2000.
- [2] K. Kinebuchi, D. D. Muresan, and T. W. Parks, "Image interpolation using wavelet-based hidden Markov trees," *Proc. ICASSP-2001*, vol. 3, pp. 7–11, May 2001.
- [3] A. Temizel, "Image resolution enhancement using wavelet domain hidden Markov tree and coefficient sign estimation," *Proc. ICIP-2007*, vol. 5, pp. 381–384, Sept. 2007.
- [4] M. Li and T. Nguyen, "Markov random field model-based edge-directed image interpolation," *Proc. ICIP-2007*, vol. 2, pp. 93–96, Sept. 2007.
- [5] J. Allebach and P. Wong, "Edge-directed interpolation," *Proc. ICIP-1996*, vol. 3, pp. 707–710, Sept. 1996.
- [6] X. Li and M. T. Orchard, "New edge-directed interpolation," *IEEE Trans. Image Processing*, vol. 10, pp. 1521–1527, Oct. 2001.
- [7] S. Grace Chang, Z. Cvetković, and M. Vetterli, "Locally adaptive wavelet-based image interpolation," *IEEE Trans. Image Processing*, vol. 15, pp. 1471–1485, June 2006.
- [8] S. Mallat and S. Zhong, "Characterization of signals from multiscale edges," *IEEE Trans. Pattern Anal. Machine Intell.*, vol. 14, pp. 2207–2232, July 1992.
- [9] S. Mallat, *A Wavelet Tour of Signal Processing*, Academic Press, San Diego, CA, 1997.
- [10] V. Velisavljević, B. Beferull-Lozano, and M. Vetterli, "Space-frequency quantization for image compression with directionlets," *IEEE Trans. Image Processing*, vol. 16, pp. 1761–1773, July 2007.
- [11] V. Velisavljević, B. Beferull-Lozano, and M. Vetterli, "Space-frequency quantization using directionlets," *Proc. ICIP-2007*, vol. 3, pp. 161–164, Sept. 2007.
- [12] M. Antonini, M. Barlaud, P. Mathieu, and I. Daubechies, "Image coding using wavelet transform," *IEEE Trans. Image Processing*, vol. 1, pp. 205–220, Apr. 1992.